TOWARDS A SHAPE MODEL OF WHITE MATTER FIBER BUNDLES USING DIFFUSION TENSOR MRI

Isabelle Corouge[1,2]*, Sylvain Gouttard*[2,3] *and Guido Gerig*[1,2]

[1]Department of Computer Science, [2]Department of Psychiatry,
University of North Carolina, Chapel Hill, NC27599, USA
[3]ESCPE Lyon, 69100 Villeurbanne, France
emails: corouge@unc.edu, sylvain.gouttard@cpe.fr, gerig@cs.unc.edu

ABSTRACT

White matter fiber bundles of the human brain form a spatial pattern defined by the anatomical and functional architecture. Human brain atlases provide names for individual tracts and document that these patterns are comparable across subjects. Tractography applied to the tensor field in diffusion tensor imaging (DTI) results in sets of streamlines which can be associated with major fiber tracts. Comparison of fiber tract properties across subjects requires comparison at corresponding anatomical locations. As an alternative to linear and nonlinear registration of DTI images and voxel-based analysis, we propose a novel methodology that models the shape of white matter tracts. A clustering uses similarity of adjacent curves and an iterative processing scheme to group sets of curves to bundles and to reject outliers. Unlike previous work which models fiber tracts as sets of curves centered around a spine, we extend the notion of bundling towards a more general representation of manifolds. We describe tracts, represented as sets of curves of similar shape, by a shape prototype swept along a space trajectory. This approach can naturally describe white matter structures observed either as bundles dispersing towards the cortex or tracts defined as dense patterns of parallel fibers forming manifolds. Curves are parameterized by arc-length and represented by intrinsic local shape properties (curvature and torsion). Feasibility is demonstrated by modeling the left and right cortico-spinal tracts and a part of the transversal callosal tract.

1. INTRODUCTION

Diffusion Tensor Imaging (DTI) of brain structures measures diffusion properties by the local probability of self-motion of water molecules. A tensor field, represented by 3×3 symmetric definite-positive matrices, characterizes amount and locally preferred directions of local diffusivity. While diffusion can be considered isotropic in fluid it appears highly anisotropic along neural fiber tracts due to inhibition of free diffusion of intra- and extra-cellular fluid. DTI has become the preferred modality to explore white matter properties associated with brain connectivity *in vivo*. To date, most research work has been dedicated to the calculation of the tensor field, its regularization, its visualization and subsequently to the design of fiber tracking algorithms [1], [2], [3], [4], [5], [6]. Some groups have investigated ways to further analyze DT images. Alexander *et al.* address matching issues in DTI [7] in order to characterize variations in white matter structure within a population. Xu *et al.* combine tractography and spatial normalization to produce statistical maps of fiber occurrence [8] while Fillard *et al.* propose to perform statistical analysis of diffusion properties along fibers [9].

In this paper, we propose a new framework for modeling and shape analysis of fibers bundles. We propose to cluster a set of fibers into meaningful bundles using various similarity metrics and to study shape deviation within these bundles with respect to a prototype. Closely related previous work has been proposed by Ding *et al.* [10]. Their bundling algorithm relies on the concept of subdivision into corresponding curve segments and the use of Euclidean distance to define piece-wise similarity. Geometric characterization is obtained by averaging shape features (e.g. curvature and torsion) along each bundle medial axis. Instead, we study the clustering fibers into bundles based on alternative distance metrics and we keep individual local shape characterization of each curve within a bundle. Ultimately, we will model bundles not only by prototypes and statistical variation but rather by a prototype shape and its space trajectory. This model would be particularly appropriate for bundles like dense callosal fibers which are observed as a "sweeping" of a U-shaped template (see Figures 1.c and 1.d).

This research is supported by the NCI grant P01 CA4792. We are grateful to C. Davatzikos, University of Pennsylvania, and S. Mori, John Hopkins University, for providing an early version of the fiber-tracking tool. We acknowledge Matthieu Jomier and Julien Jomier, both UNC-Chapel Hill, for their precious help and fruitful discussions.

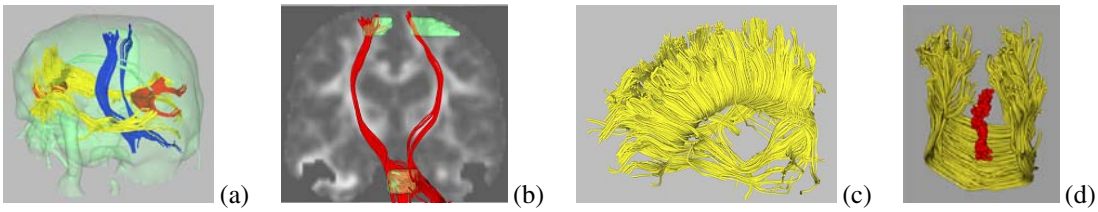

Fig. 1. Examples of fibers obtained from high-resolution DTI by tractography. (a) Major fiber tracts: cortico-spinal (blue), superior longitudinal (yellow), splenium/genu (red); (b) cortico-spinal tract (red) with source and target regions of interest (green); (c) about 8000 callosal fibers; (d) subset of (c) suggesting the new bundling concept proposed here: this bundle could be represented as a U-shaped prototype shape and its trajectory, here the center of mass of each curve (red dots).

2. METHODS

2.1. Preprocessing: fiber extraction

The extraction of fiber tracts is performed with the tractography tool described in [6]. The tensor field is computed from high-resolution DTI data (baseline and 6 directional channels with $2 \times 2 \times 2$ mm^3 resolution) by solving the Stejskal-Tanner's diffusion equation system as described in [1]. Streamlines following the principal diffusion tensor directions between source and target regions of interest are then extracted by tractography under local continuity constraints [8]. Except at branchings or crossings, these 3D curves are assumed to represent the most likely paths through the tensor field and to mimick white matter pathways. Figure 1 shows fiber sets extracted by this method. Note that the term *fibers* used here is representing streamlines extracted from the tensor field. These do not represent single fibers but coarse-scale properties of fiber bundles.

2.2. Clustering fibers to bundles

The fiber tracking process provides us with a set $\mathcal{F}$ of 3D curves, F_i, each represented by a set of 3D points $\mathbf{p}_k$, $\mathcal{F} = \{F_i, F_i = \{\mathbf{p}_k\}\}$. Due to limited robustness of fiber tracking at junctions and in noisy low-contrast regions, $\mathcal{F}$ may still contain outlier curves. Also, the set of reconstructed fibers might contain curves that are part of other anatomical bundles. We therefore develop an algorithm to remove outliers and to cluster curves to bundles. We propose a clustering algorithm based on position and shape similarity of pairs of fibers and test several distance metrics.

Given a pairwise distance d and a fiber F_i, d is computed between F_i and F_j for all F_j in $\mathcal{F}$, $j \neq i$. F_i and F_j are decided to be in the same class if $d(F_i, F_j) < t$ where $t \in \mathbb{R}$ is a treshold to be chosen. Clusters of very low cardinal (e.g. containing less than 10% of initial fibers) are considered as outliers and rejected. Thus, for each fiber F_i within a class $\mathcal{C}$, at least one fiber $F_j, j \neq i$ in $\mathcal{C}$ is such that $d(F_i, F_j) < t$. After calculating a table of pairwise distances, the algorithm propagates labels from neighbouring fiber to neighbouring fiber and benefits from a "transitivity property". Moreover, only one parameter, the threshold t, has to be set up. A large value of t implies a low number of classes, whereas a smaller value will result in an increased number of classes. The optimal parameter t depends on the data set under examination and on the choice of the distance metric. We compute the histogram of the number of classes as a function of t to study the sensitivity of each metric in regard to this parameter and to help users to come up with a meaningful choice. For example, users select the number of sought clusters instead of the parameter itself.

Three pairwise distances between fibers F_i and F_j have been implemented:

1. Closest point distance, d_c:
$$d_c(F_i, F_j) = \min_{\mathbf{p}_k \in F_i, \mathbf{p}_l \in F_j} \| \mathbf{p}_k - \mathbf{p}_l \|, \quad (1)$$
$\| \cdot \|$ being the Euclidean norm;

2. Mean distance of closest distances called d_M and defined as:
$$d_M(F_i, F_j) = \text{mean}(d_m(F_i, F_j), d_m(F_j, F_i))$$
$$\text{with } d_m(F_i, F_j) = \text{mean}_{\mathbf{p}_l \in F_i} \min_{\mathbf{p}_k \in F_j} \|\mathbf{p}_k - \mathbf{p}_l\|, \quad (2)$$

3. Hausdorff distance, d_H:
$$d_H(F_i, F_j) = \max(d_h(F_i, F_j), d_h(F_i, F_j))$$
$$\text{with } d_h(F_i, F_j) = \max_{\mathbf{p}_k \in F_i} \min_{\mathbf{p}_l \in F_j} \|\mathbf{p}_k - \mathbf{p}_l\|. \quad (3)$$

Additionally, we use shape-based distances by extracting geometric characteristics from fibers such as length, center of mass and second order moments. The principle of the clustering algorithm remains the same when using first or second order moments. In the former case, d is the Euclidean distance between centers of mass, called d_G, whereas in the latter case it represents orientation similarity of the first principal directions.

The distance d_c can not be expected to have a good discrimination power between fibers since it encodes only very coarse information about fiber similarity and closeness. On the contrary, d_M provides a global similarity measure integrated along the whole curve. The Hausdorff distance being a worst-case distance, it is a useful metric to reject outliers and prevents the algorithm from clustering curves with high dissimilarity. Centers of mass are an appropriate feature to measure coarse similarity of pose since they are a first order complete representation of a fiber, whereas the second

Fig. 2. Coronal and sagittal 3D views of the test data sets. Left: 40 fibers presenting left and right cortico-spinal tracts. Right: 500 callosal fibers.

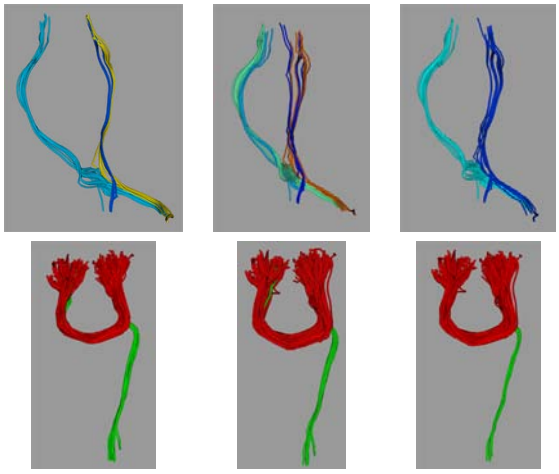

Fig. 3. From left to right: clustering to bundles obtained with distance metrics d_M, d_H and d_G on the cortical-spinal tracts (top) and callosal fibers (bottom) shown in Figure 2.

order moment metric has difficulties to discriminate dense fiber sets (see for example Figure 1.c) because of their high sensitivity to noise.

2.3. Shape analysis of fiber bundles

Our main goal is a modeling of white matter bundles including a geometric characterization. Qualitative views of 3D rendering suggest that sets of fibers might be described as a replication of a prototype curve along a space trajectory, simulating the sweeping of a space curve to form a manifold. We propose to generate a geometric description of a set of curves forming a bundle, to calculate an average, prototype curve, and to analyze the variability of shape deviations from this prototype. Local shape descriptors are derived from the Frénet frame.

Given a differentiable parameterization $r(t)$ of a curve $\mathcal{C}$, the Frénet frame $(\overrightarrow{T}, \overrightarrow{N}, \overrightarrow{B})$ in each point $\mathbf{p}$ of the curve is defined by:

$$\begin{cases} \overrightarrow{T} = \frac{r'(t)}{\|r'(t)\|} & \text{where } r'(t) = \frac{d}{dt} r(t) \\ \overrightarrow{N} = \frac{\overrightarrow{T}'}{\|\overrightarrow{T}'\|} & \text{where } \overrightarrow{T}' = \frac{d\overrightarrow{T}}{dt} \\ \overrightarrow{B} = \overrightarrow{T} \wedge \overrightarrow{N} & \text{where } \wedge \text{ denotes the vector product.} \end{cases} \quad (4)$$

The vector $\overrightarrow{T}$ is the unit tangent vector, $\overrightarrow{N}$ the unit normal vector and $\overrightarrow{B}$ supplements the frame so that it is orthonormal. At each point $\mathbf{p}$, this frame allows the calculation of local features such as curvature κ and torsion τ. These measurements are given by the Serret-Frénet formulæ:

$$\frac{d\overrightarrow{T}}{ds} = \kappa\overrightarrow{N} \quad \text{and} \quad \frac{d\overrightarrow{B}}{ds} = -\tau\overrightarrow{N} \quad (5)$$

where s is the curvilinear abscissa of $\mathcal{C}$.

In order to perform an analysis of these features across fibers, we design a simple matching scheme that establishes point correspondences between fibers. First, we define a common origin for the set of fibers in each cluster. The choice of this origin might be based on geometric criteria, e.g. a cross-section with minimal area, or based on anatomical information, like the symmetry plane of the interhemispheric fissure. Second, we reparameterize the fibers with cubic B-splines wich enables an equidistant sampling of all curves in the training set and also allows an adequate sampling of fibers with different overall lengths. Points having the same curvilinear abscissæ across the fiber set are defined as homologuous. Curvature and torsion are computed along each curve as described above. Pointwise mean and standard deviation on these features define average and variability, characterizing local shape of the whole bundle.

3. EXPERIMENTS AND RESULTS

Figure 2 shows 3D views of the two test data sets. The first represents the cortico-spinal tracts of the left and right hemispheres. The second corresponds to a dense set of callosal fibers also including parts of the inferior-posterior pathways. Both data sets contain many outliers. Note for example the presence of outlier curves crossing the interhemispheric plane in Figure 2, left. Figure 3 presents bundles obtained with distance metrics d_M, d_H and d_G. These results compare the power of the different metrics to cluster curves to bundles and to remove outliers.

Shape analysis of bundles uses the filtered sets of curves as shown in Figure 4, top. The common origin of all fibers for the cortico-spinal tracts is chosen as the location of thinnest cross-section at the level of the internal capsule. For the callosal fiber bundle, a natural choice is the intersection with the mid-sagittal plane. Figure 4 top displays the shape features of the set of curves aligned to bundles. Due to limited available space, only curvature is displayed but similar properties are observed as torsion is concerned. The bottom figure shows mean and standard deviation of curvature for both test cases. The corticospinal tract (left figure) shows two parts of increased variability, located at the locations of largest curvature. The curves seem to be well aligned and demonstrate very similar shape features. The callosal tract composed of over 350 curves (right figure) also seems to demonstrate that the curves present very similar shape features across the corpus callosum. The 3D rendering of the

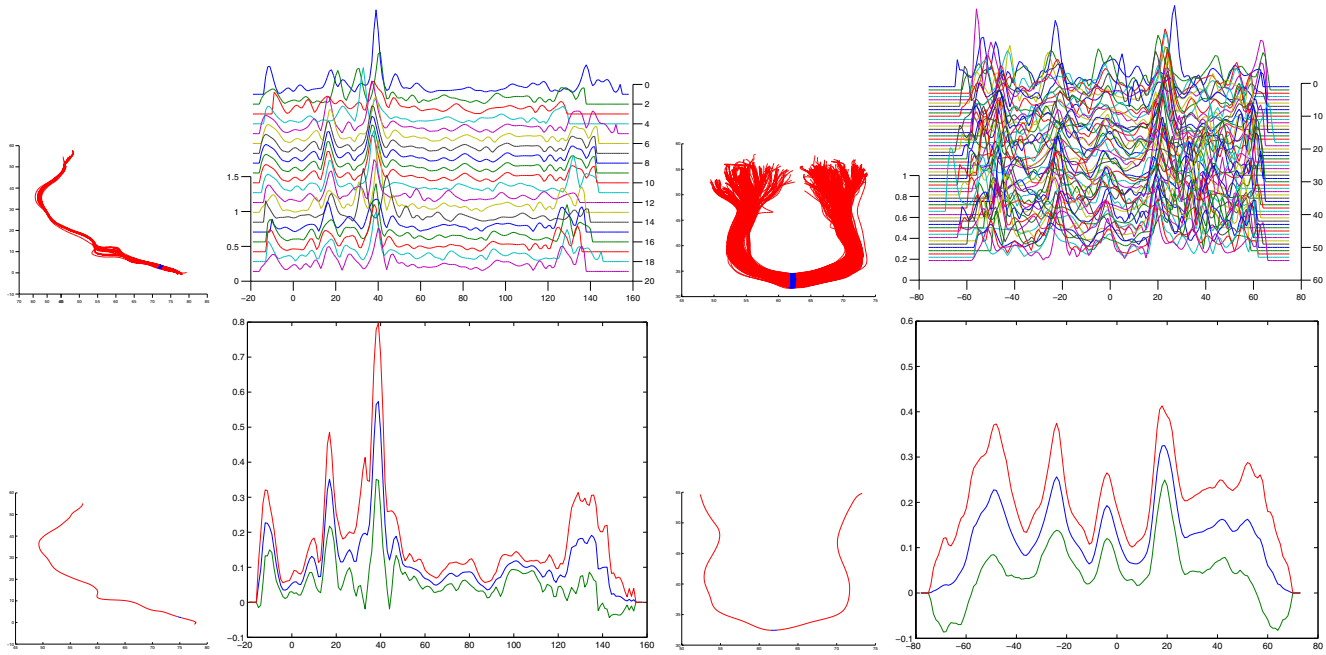

Fig. 4. Two test data sets: Top: 3D rendering with coordinate origin (blue) and curvature of the aligned set of fibers. Bottom: prototype shape and statistics of curvature with mean (blue) and standard deviation (red and green).

set of curves demonstrates that these fibers follow a common shape originating at the center and then dispersing towards the cortex. This process is clearly shown in the curvature plot, where a central portion bounded by low curvature parts (coordinates -40 to 30) presents lower variability in comparison to both ends of the curves.

4. CONCLUSION

This paper presents new techniques for clustering 3D curves to bundles, to remove outlier curves and to develop a technique towards shape description of these bundles. The preliminary results on two test datasets demonstrate that the new clustering process is quite efficient to bundle sets of curves to anatomically meaningful fiber tracts. This is further confirmed in our comparison of local shape features across the set of curves. The main goal is the development of a new methodology for modeling white matter tracts of the human brain, given diffusion tensor images. Our general model of bundles takes into account that white matter tracts are not observed as "cables" composed of sets of curves centered around a spine, but as "ribbon cables" that form thin manifolds. Further, fiber tracts might fan out and disperse due to their function of connecting folded cortical regions with large surface area, collecting these fibers to thin, dense bundles through the brain (e.g. towards the brain stem or through the central part of the brain for longitudinal fasciculi). Our future work will focus to extend this shape model to get a full description of the prototype shape, its change along a trajectory, and a shape description of the trajectory curve with associated smooth change of the local coordinate frame.

5. REFERENCES

[1] C.-F. Westin, S.E. Maier, H. Mamata, A. Nabavi, F.A. Jolesz, and R. Kikinis, "Processing and visualization for diffusion tensor MRI," *MedIA*, vol. 6, pp. 93–108, 2002.

[2] O. Coulon, D.C. Alexander, and S.R. Arridge, "A regularization scheme for diffusion tensor magnetic resonance images," in *IPMI*, 2001, LNCS, pp. 92–105.

[3] P.J. Basser, S. Pajevic, C. Pierpaoli, and A. Aldroubi, "Fiber tract following in the human brain using DT-MRI data," *IEICE Trans. on Information and Systems*, vol. E85-D, no. 1, pp. 15–21, 2002.

[4] M. Björnemo, A. Brun, R. Kikinis, and C.-F. Westin, "Regularized stochastic white matter tractography using diffusion tensor MRI," in *MICCAI*, 2002, vol. 2488 of *LNCS*, pp. 435–442.

[5] L. Zhukov and A.H. Barr, "Oriented tensor reconstruction: tracing neural pathways from diffusion tensor MRI," in *IEEE Visualization*, 2002.

[6] P. Fillard and G. Gerig, "Analysis tool for diffusion tensor MRI," in *MICCAI*, 2003, vol. 2879 of *LNCS*, pp. 967–968.

[7] D.C. Alexander and J.C. Gee, "Elastic matching of diffusion tensor images," *CVIU*, vol. 77, pp. 233–250, 200.

[8] D. Xu, S. Mori, M. Solaiyappan, P.C.M. van Zijl, and C. Davatzikos, "A framework for callosal fiber distribution analysis," *NeuroImage*, vol. 17, pp. 1131–1143, 2002.

[9] P. Fillard, J. Gilmore, W. Lin, and G. Gerig, "Quantitative analysis of white matter fiber properties along geodesic paths," in *MICCAI*, 2003, vol. 2879 of *LNCS*, pp. 16–23.

[10] Z. Ding, J.C. Gore, and A.W. Anderson, "Classification and quantification of neuronal fiber pathways using diffusion tensor MRI," *Magn. Res. Med.*, vol. 49, pp. 716–721, 2003.